

Published in final edited form as:

*Gastroenterology*. 2014 April ; 146(4): 1028–1039. doi:10.1053/j.gastro.2014.01.015.

## Mutations in Tetratricopeptide Repeat Domain 7A Result in a Severe Form of Very Early Onset Inflammatory Bowel Disease

Yaron Avitzur<sup>1,2,3,\*,\$</sup>, Conghui Guo<sup>\*.2,\$</sup>, Lucas A Mastropaolo<sup>2,\$</sup>, Ehsan Bahrami<sup>4</sup>, Hannah Chen<sup>5</sup>, Zhen Zhao<sup>2</sup>, Abdul Elkadri<sup>2,3,6,\$</sup>, Sandeep Dhillon<sup>2,\$</sup>, Ryan Murchie<sup>2,\$</sup>, Ramzi Fattouh<sup>2,\$</sup>, Hien Huynh<sup>7,\$</sup>, Jennifer L Walker<sup>8</sup>, Paul W Wales<sup>1</sup>, Ernest Cutz<sup>9</sup>, Yoichi Kakuta<sup>10</sup>, Joel Dudley<sup>11</sup>, Jochen Kammermeier<sup>12</sup>, Fiona Powrie<sup>13,\$</sup>, Neil Shah<sup>12</sup>, Christoph Walz<sup>14</sup>, Michaela Nathrath<sup>15</sup>, Daniel Kotlarz<sup>4</sup>, Jacek Puchaka<sup>4</sup>, John Krieger<sup>2</sup>, Tomas Racek<sup>4</sup>, Thomas Kirchner<sup>14</sup>, Thomas D Walters<sup>2,3,\$</sup>, John H Brumell<sup>2,3,6,\$</sup>, Anne M Griffiths<sup>2,3,\$</sup>, Nima Rezaei<sup>16,17</sup>, Parisa Rashtian<sup>18</sup>, Mehri Najafi<sup>18</sup>, Maryam Monajemzadeh<sup>19</sup>, Stephen Pelsue<sup>8</sup>, Dermot PB McGovern<sup>10,\$</sup>, Holm H Uhlig<sup>5,\$</sup>, Eric Schadt<sup>11,\$</sup>, Christoph Klein<sup>\*.4,\$</sup>, Scott B Snapper<sup>\*.20,\$</sup>, and Aleixo M Muise<sup>2,3,6,\*,\$,^</sup>

<sup>1</sup>Group for Improvement of Intestinal Function and Treatment (GIFT), Hospital for Sick Children, Toronto, Ontario, Canada

<sup>2</sup>SickKids Inflammatory Bowel Disease Center and Cell Biology Program, Research Institute, Hospital for Sick Children, Toronto, ON, Canada

<sup>3</sup>Division of Gastroenterology, Hepatology, and Nutrition, Department of Pediatrics, University of Toronto, Hospital for Sick Children, Toronto, ON, Canada

<sup>4</sup>Department of Pediatrics, Dr. von Hauner Children's Hospital, Ludwig-Maximilians-University, Munich, Germany

<sup>5</sup>Translational Gastroenterology Unit and Paediatric Gastroenterology, University of Oxford, Oxford, UK

<sup>6</sup>Institute of Medical Science, University of Toronto, Toronto, ON, Canada

<sup>7</sup>Division of Pediatric Gastroenterology, Stollery Children's Hospital, Edmonton, ON, Canada

<sup>8</sup>Department of Immunology & Molecular Biology, University of Southern Maine, Maine

<sup>9</sup>Division of Pathology, The Hospital for Sick Children, Toronto, Canada

© 2014 The American Gastroenterological Association. Published by Elsevier Inc. All rights reserved.

<sup>^</sup>Address Correspondence to: Aleixo Muise, 555 University Ave., The Hospital for Sick Children, Toronto, ON, Canada, M5G 1X8, aleixo.muise@utoronto.ca, Phone: 416-813-7735, Fax: 416-813-6531.

<sup>§</sup>interNational Early Onset Pediatrics IBD Cohort Study ([www.NEOPICS.org](http://www.NEOPICS.org))

<sup>\*</sup>Contributed equally and should be considered aequo loco

Conflict of Interest: none

Author Contribution: YM, CG, LAM, EB, HC, ZZ, AE, SD, RM, RF, JW, JK, YK, JD, and DK carried out the research carried out here under the supervision of JHB, FP, AMD, SP, DPBG, HHU, ES, SBS, CK, and AMM. PWW, NS, CW, MN, JP, TR, TK, EC, TDW, AMG, YA, NR, PR, and MN provided clinical care. AMM wrote the manuscript with assistance from all authors.

**Publisher's Disclaimer:** This is a PDF file of an unedited manuscript that has been accepted for publication. As a service to our customers we are providing this early version of the manuscript. The manuscript will undergo copyediting, typesetting, and review of the resulting proof before it is published in its final citable form. Please note that during the production process errors may be discovered which could affect the content, and all legal disclaimers that apply to the journal pertain.

<sup>10</sup>F. Widjaja Foundation Inflammatory Bowel Disease Center and Immunobiology Research Institute at Cedars-Sinai Medical Center, Los Angeles

<sup>11</sup>Institute for Genomics and Multiscale Biology, Department of Genetics and Genomics Sciences, Mount Sinai NY

<sup>12</sup>Gastroenterology Department, Great Ormond Street Hospital, London, UK

<sup>13</sup>Translational Gastroenterology Unit, Nuffield Department Clinical Medicine-Experimental Medicine Division, University of Oxford, John Radcliffe Hospital, Oxford, UK

<sup>14</sup>Institute for Pathology, Ludwig-Maximilians University, Munich, Germany

<sup>15</sup>Department of Pediatric Oncology, Kassel and CCG Osteosarcoma, Helmholtz Center Munich, Germany

<sup>16</sup>Research Center for Immunodeficiencies, Children's Medical Center, Tehran University of Medical Sciences, Tehran, Iran

<sup>17</sup>Molecular Immunology Research Center; and Department of Immunology, School of Medicine, Tehran University of Medical Sciences, Tehran, Iran

<sup>18</sup>Department of Pediatric Gastroenterology, Children's Medical Center, Tehran University of Medical Sciences, Tehran, Iran

<sup>19</sup>Department of Pathology, Children's Medical Center, Tehran University of Medical Sciences, Tehran, Iran

<sup>20</sup>Division of Pediatric Gastroenterology, Hepatology, and Nutrition, Department of Medicine, Children's Hospital Boston; Division of Gastroenterology and Hepatology, Brigham & Women's Hospital, Department of Medicine, Harvard Medical School, Boston, MA

## Abstract

**Background & Aims**—Very early onset inflammatory bowel diseases (VEOIBD), including infant disorders, are a diverse group of diseases found in children less than 6 years of age. They have been associated with several gene variants. We aimed to identify genes that cause VEOIBD.

**Methods**—We performed whole-exome sequencing of DNA from 1 infants with severe enterocolitis and her parents. Candidate gene mutations were validated in 40 pediatric patients and functional studies were carried out using intestinal samples and human intestinal cell lines.

**Results**—We identified compound heterozygote mutations in the tetratricopeptide repeat domain 7 (*TTC7A*) gene in an infant from non-consanguineous parents with severe exfoliative apoptotic enterocolitis; we also detected the mutations in 2 unrelated families, each with 2 affected siblings. *TTC7A* interacts with EFR3 homolog B (*EFR3B*) to regulate phosphatidylinositol 4-kinase (*PI4KA*) at the plasma membrane. Functional studies demonstrated that *TTC7A* is expressed in human enterocytes. The mutations we identified in *TTC7A* result in either mislocalization or reduced expression of *TTC7A*. *PI4KA* was found to co-immunoprecipitate with *TTC7A*; the identified *TTC7A* mutations reduced this binding. Knockdown of *TTC7A* in human intestinal-like cell lines reduced their adhesion, increased apoptosis, and decreased production of phosphatidylinositol 4-phosphate.

**Conclusion**—In a genetic analysis, we identified loss of function mutations in *TTC7A* in 5 infants with VEOIBD. Functional studies demonstrated that the mutations cause defects in enterocytes and T cells that lead to severe apoptotic enterocolitis. Defects in the PI4KA–TTC7A–EFR3B pathway are involved in the pathogenesis of VEOIBD.

## Keywords

IBD; intestinal atresia; autoimmunity; intestine

---

Very Early Onset Inflammatory Bowel Diseases (VEOIBD), including forms of infantile disease, are a diverse group of diseases that are diagnosed prior to 6 years of age<sup>1</sup>. In contrast to adult onset IBD, VEOIBD frequently encompasses a unique clinical presentation with severe, colonic disease that often has poor response to standard therapies including biologic agents<sup>2, 3</sup>. Recently, several groups, including our own, demonstrated that mutations in *IL10RA/B* genes<sup>4</sup> cause a severe form of VEOIBD, with symptoms consistently developing in infancy<sup>5</sup>. Subsequently, causative variants in *IL10*<sup>6</sup>, *XIAP*<sup>7</sup>, *ADAM17*<sup>8</sup>, and *NCF4*<sup>9</sup>, and association variants in the NADPH oxidase genes *NCF2/RAC2*<sup>10</sup> were identified in VEOIBD patients suggesting that severe infantile colitis frequently starting immediately after birth can represent a group of heterogeneous monogenetic diseases.

Recently mutations in the *TTC7A* gene were found to cause multiple intestinal atresia (MIA) with severe combined immune deficiency (SCID) although no details regarding the intestinal phenotype or function of the *TTC7A* gene were provided<sup>11, 12</sup>. In this report we describe novel human mutations in the *TTC7A* gene (we termed *TTC7A*-deficiency) identified independently by whole exome sequencing that result in severe infantile apoptotic enterocolitis with and without MIA and define the intestinal defects associated with this novel form of VEO-IBD.

## METHODS

### Whole exome sequencing

Genetic studies were carried out with approval from the research ethics board at the Hospital for Sick Children, University of Oxford, Cedars-Sinai Medical Center, and Dr. von Hauner Children's Hospital, LMU Munich. In the Index Case whole exome sequencing (WES) was performed using the Agilent SureSelect Human All Exon 50Mb kit with high-throughput sequencing conducted using the Solid 4 System at The Center for Applied Genomics (TCAG) through the Hospital for Sick Children (Toronto, ON) on the complete parent-child trio set. Sanger sequencing was used to verify variant genotypes in the index patient and her family and 40 infantile patients from the institutions named above were screened for *TTC7A* mutations.

**Histological Methods** are found in the Supplemental Material.

### Tandem Mass Spectrometry

Detailed methods are found in the Supplemental Materials. Briefly, to identify potential interactors of *TTC7A*, M2 anti-FLAG-agarose FLAG-agarose FLAG-tagged WT, E71K or

Q526X TTC7A were transiently overexpressed in HEK293T, immunoprecipitated with FLAG-agarose, and bound proteins were trypsin digested and analyzed by tandem mass spectrometry as previously described<sup>13</sup>.

### Knockdown of Endogenous TTC7A by shRNA

GIPZ human TTC7A shRNA (GFP tagged) targeting coding regions and GFP tagged control shRNA (Thermo Scientific, USA) were transfected into Henle-407 cells with Lipofectamine 2000 (Life Technologies, USA). Detailed methods are found in the Supplemental Materials.

### Apoptosis Analysis

Confluent cells were starved for indicated time points. Apoptosis was assessed by both measured Caspase-3 using western blotting and cytoplasmic DNA fragments using flow cytometric analysis of AnnexinV. Cells were stained with AnnexinV-PE and 7-AAD (BD Biosciences, USA) according to manufacturer's instructions and samples were run on a BD LSR II analyze. Apoptotic cells were identified as AnnexinV<sup>+</sup> 7-AAD<sup>-</sup> cells.

### Cell Adhesion Assay

To evaluate cellular adhesion,  $\approx 5 \times 10^4$  cells were seeded on 96-well plates pre-coated with fibronectin (20  $\mu\text{g/ml}$ ; Sigma-Aldrich, USA), collagen type I (50  $\mu\text{g/ml}$ ; Life Technologies, USA), or bovine serum albumin (5% in phosphate buffered saline (PBS); Sigma, USA) for 60 min at 37°C. The wells were subsequently washed with PBS twice to remove non-adherent cells. After fixation with 4% paraformaldehyde, attached cells were visualized by staining with 1% crystal violet dissolved in 33% acetic acid and were quantified by measuring the absorbance at 570nm on a Versamax microplate reader (Molecular devices, USA).

### Constructs, Western Blot, Cell culture, and Immunoprecipitation

Details of constructs, antibodies, and methods used can be found in the Supplemental Methods.

### Statistical Analysis

Data are presented as mean  $\pm$  SD. Experiments were performed with a minimum of three replications. Statistical significance between groups was established at  $p < 0.05$  using a two-tailed Student's *t*-test. *P* values are indicated in the figure legend and text.

## RESULTS

### Identification of Apoptotic Enterocolitis in a VEOIBD Patient

In Family-1 (Index Case), a female patient born at term to a Caucasian mother and Sudanese father presented with high output secretory diarrhea and hematochezia starting almost immediately after birth requiring total parenteral nutrition. Colonoscopy demonstrated chronic inflammation with severe friability, exfoliative mucosal changes, and sloughed mucosa within the colonic lumen (Figure 1A). Biopsies taken from the duodenum showed

villous atrophy and the duodenum and colon showed glandular dropout with crypt apoptosis and exploding crypts (Figure 1B–C). The severity of the epithelial injury was strikingly reminiscent of acute gastrointestinal graft-versus-host disease and intestine allograft rejection. There was no evidence of perianal disease, dermatological disease. The patient had clinical features of immunodeficiency including lymphopenia and hypogammaglobulinemia. The patient was treated with 2 mg/kg methylprednisone without significant response. At 11 months of age, she developed respiratory failure and succumbed shortly afterwards (see Supplemental Material for details). Autopsy did not show any evidence of bowel atresia but confirmed widespread severe apoptotic enterocolitis as previously identified by endoscopy.

In Family-2, an infant male was born at 36 weeks gestation to non-consanguineous Caucasian parents. Shortly after birth the infant presented with symptoms of small bowel obstruction due to short segment jejunal atresia. Despite surgical resection, the intestinal disease progressed and the patient was found to have recurrent multiple atretic areas that also required resection. The disease continue to progress and the patient died of cardiac arrest prior to three months of age. A second child from the same family also had jejunal atresia at birth that was initially resected. The intestinal disease progressed ultimately resulting in the patient's death at the age of 19 months. Both children had evidence of immunodeficiency with lymphopenia and T-cell deficiency. Pathological analysis showed loss of intestinal architecture, focal scarring, and severe inflammation with increased apoptosis reminiscent of graft-versus-host-disease as described in Family-1 (Figure 1D–E).

Family-3 had two infant daughters from consanguineous parents who presented with diarrhea and failure to thrive shortly after birth. Both children had no evidence of overt immunodeficiency and pathological analysis of colonic biopsies showed similar loss of intestinal architecture, focal scarring, and severe inflammation with increased enterocyte apoptosis (Figure 1F) and areas where surface epithelium was detached as described in Families 1 and 2. The younger girl died before the age of 1 year due to uncontrolled candida sepsis and the older girl is presently partially treated with TPN (see Supplemental Material for details; Summarized in Table 1).

### Whole Exome Sequencing

Whole exome sequencing of Family-1 resulted in greater than 80 times coverage of exomes and the subsequent identification of a non-synonymous variant in exon 2 inherited from the father, and a nonsense mutation in exon 14 inherited from the mother in the Tetratricopeptide Repeat Domain 7A (*TTC7A*) gene (Figure 2A). The non-synonymous mutation in exon 2 at c.211 G>A resulted in a glutamic acid to lysine substitution at amino acid position 71 (p.E71K; rs147914967). The mutant allele is not found in either the NCBI or 1000 genomes databases, and only found in one heterozygous allele from 6503 healthy individuals genotyped in the NHLBI Exome Sequencing Project (<http://evs.gs.washington.edu>). The mutation was predicted to be highly deleterious with a Polyphen<sup>14</sup> score of 0.99 and located in a highly conserved alpha-helical region (Figure 2D and Supplemental Figure 1). The second *TTC7A* mutation in exon 14 at c.1944 C>T transition resulted in a nonsense mutation causing the premature termination of the protein at

amino acid 526 (p.Q526X). This nonsense mutation has not been previously described in the aforementioned datasets.

In siblings from Family-2 with severe apoptotic enterocolitis, we also identified heterozygous *TTC7A* mutations. The c.844-1 G>T mutation in the splice acceptor site of exon 7 was inherited from the mother and a c.1204-2 A>G mutation in splice acceptor site of exon 10 was inherited from the father (Figure 2B). These *TTC7A* mutations were predicted to result in loss of the splice acceptor sites for both exons 7 and 10 leading to skipping of both exon 7 and 10 respectively and cause premature stop codons that would disrupt TPR domains (Figure 2D). These splice mutations have not been previously described in the aforementioned datasets and it is likely that these mutations will result in nonsense mediated decay of the *TTC7A* mRNA.

In siblings from Family-3 with severe apoptotic enterocolitis, we identified a homozygous non-synonymous mutation in exon 20 at c.2494 G>A (Figure 2C) that resulted in a alanine to threonine substitution at amino acid position 832 (p.A832T). The mutation was predicted to be highly deleterious with a Polyphen<sup>14</sup> score of 0.99 and located in a highly conserved region of the 9<sup>th</sup> TPR domain (Figure 2D; Supplemental Figure 1) and has not been previously described in the aforementioned datasets (Summarized in Table 1).

### Functional Analysis of *TTC7A* mutations in Enterocytes

Immunostaining of *TTC7A* from healthy human control intestinal tissue (Duodenum, Ileum, and Colon) showed that *TTC7A* was strongly expressed in enterocytes with areas of discreet localization at the plasma membrane and only few lamina propria cells stained positive (Figure 3A). This observed pattern of intestinal expression suggests a primary role for *TTC7A* in enterocyte homeostasis. To determine if the mutation identified in Families-1 and -3 resulted in abnormal *TTC7A* cellular localization, we transiently transfected Caco-2 cells with Myc-tagged wild type, E71K, Q526X, and A832T *TTC7A*. Immunostaining using anti-Myc antibody demonstrated that E71K, Q526X, and A832T *TTC7A* mutants appeared to accumulate in cytoplasmic puncta, whereas the WT-*TTC7A* localized diffusely in the cytoplasm (Figure 3B). Furthermore, biopsies from Family-2 patient with the *TTC7A* splice acceptor site mutations predicted to result in complete loss of the protein, as expected showed loss of *TTC7A* in enterocytes indicating that these mutations may result in nonsense mediated decay of the *TTC7A* mRNA (Figure 3C).

Knockdown of *TTC7A* by shRNA resulted in loss of cobblestone morphology, typical of human Henle 407 cells with the development of fibroblastoid morphology with spindle-like features (Figure 3D and Supplemental Figure 2). Furthermore, overexpression of E71K, A832T, and Q526X *TTC7A* in Caco-2 cells demonstrated cytoplasmic accumulations of Myc-*TTC7A* in addition to disrupted cortical actin staining suggestive of adhesion defects or loss of cellular polarity (Supplemental Figure 3). Reduced expression of *TTC7A* in the enterocytes also resulted in detachment during trypsinization (Figure 4A), impaired adhesion to collagen and fibronectin (Figure 4B), and increased apoptosis as measured by Caspase-3 (Figure 4C) and Annexin V (Figure 4D). These cellular changes are reminiscent of the apoptosis and mucosal exfoliation described in our patient.

## TTC7A Binding Partners

Tandem mass spectrometry (MS/MS) was performed on proteins co-immunoprecipitated (co-IP) from HEK293T cells expressing human TTC7A, with the aim of identifying TTC7A binding partners. Isolated proteins were digested with trypsin to generate peptide fragments and analyzed by MS/MS (Supplemental Figure 4). To refine this list to TTC7A binding partners, spectral hit counts were compared between wild-type TTC7A and the E71K mutation samples, and determined that PI4KIII $\alpha$  protein fragments were able to co-IP with wild type TTC7A but were significantly reduced with E71K TTC7A mutation (Figure 5A and Supplemental Figure 4). This PI4KIII $\alpha$  and TTC7A interaction was supported by a weighted coexpression network<sup>15</sup> from small bowel gene expression data demonstrating that *Ttc7a* falls within a subnetwork (module) of the mouse small bowel network that included *Pi4kca* (murine form of PI4KIII $\alpha$ ) (Supplementary Table 1–4; Supplementary Figure 5). The additional hits identified in the tandem mass spectrometry screen (Supplemental Figure 4) implicated several proteins associated with ubiquitination pathways, including E3 ligases (HUWE1, HECTD1, UBR5), and proteins that function in the ubiquitin-proteasome system (USP9X, PSMD1, VCP).

## Loss of TTC7A Results in PI4KIII $\alpha$ Dysfunction

As TTC7A has been previously implicated in PI4KIII $\alpha$  regulation in yeast<sup>16, 17</sup> and confirmed through the tandem mass spectrometry and network analysis of mouse small bowel, we next confirmed through co-immunoprecipitation (co-IP) experiments that TTC7A and PI4KIII $\alpha$  interacted in human cell lines. We found that Myc-Flag-tagged wild-type TTC7A was able to co-IP PI4KIII $\alpha$  indicating that these proteins interact either directly or indirectly in a larger complex (Figure 5B). We also observed reduced co-IP of PI4KIII $\alpha$  with the TTC7A Q526X and E71K mutated proteins identified in Family-1 and the A832T TTC7 mutation identified in Family-3 (Figure 5B). As the splice variants identified in Family-2 were assumed to be unstable, we would predict that the gene product of these *TTC7A* mutations would also not bind to PI4KIII $\alpha$ .

We next examined human PI4KIII $\alpha$  in intestinal tissue of healthy controls and found that PI4KIII $\alpha$  was abundantly expressed in both enterocytes and immune cells including lymphocytes (Figure 5C; Left Panel). In our patients with TTC7A-deficiency the severe disruption of the bowel architecture with sloughing of the majority of enterocytes made interpretation of PI4KIII $\alpha$  localization difficult; however, in areas with relatively preserved epithelial architecture, we observed overall reduced PI4KIII $\alpha$  expression in a patient from Family-2 (while lamina propria expression was preserved, Figure 5C). To confirm these results, we transiently co-transfected TTC7A and TTC7A shRNA into Henle-407 cells and observed a reduction in PI4KIII $\alpha$  (Figure 5D–E). These results indicate that loss of TTC7A resulted in aberrant sub-cellular localization of PI4KIII $\alpha$  in enterocytes.

Finally we determined that knockdown of TTC7A in human Henle-407 cell lines resulted in decreased phosphatidylinositol 4-phosphate (PI-4P), the end product of PI4KIII $\alpha$  enzyme, in both the cytoplasm (Figure 5F) and at the plasma membrane (Figure 5G). Together these results indicate that TTC7A is required for PI4KIII $\alpha$  localization to the plasma membrane and that TTC7A-deficiency result in loss of PI4KIII $\alpha$  signaling in enterocytes.

## DISCUSSION

Our Index Case (Family-1) had severe infantile apoptotic enterocolitis with a presentation significantly different from previously described cases of VEOIBD with *IL10* and *IL10R* mutations that invariably present with colitis and perianal disease<sup>4, 5, 18–20</sup>. The severe enterocolitis with friability and exfoliative mucosal changes along with villous atrophy, gland dropout and crypt apoptosis led to our genetic exploration through whole exome sequencing and the identification of *TTC7A* as the causative gene.

The tetratricopeptide repeat (TPR) domain is defined by a degenerate consensus sequence of 34 amino acids<sup>21</sup> and four of the five *TTC7A* mutations found in our patients resulted in disruption of these TPR domains. TPR domains mediate protein-protein interactions and the assembly of multi-protein complexes that are involved in the regulation of cell cycle, transcription, and protein transport<sup>22</sup>. Our tandem mass spectrometry and intestinal network experiments demonstrated an association between *TTC7A* and PI4KIII $\alpha$  that was previously only described in yeast<sup>16, 17</sup>. In yeast the *TTC7* ortholog, *YPP1*, is essential and has been shown to rescue a lethal  $\alpha$ -synuclein ( $\alpha$ Syn-A53T) yeast mutant<sup>23</sup>. Ypp1 (*TTC7*) directly binds to Stt4 (PI4KIII $\alpha$ ) and this binding is critical to maintain Phosphatidylinositol 4-phosphate (PIP) levels and PI4KIII $\alpha$  stability at the plasma membrane<sup>16, 17</sup>. Moreover, in yeast, the phenotypes of *YPP1* (*TTC7*) and *STT4* (PI4KIII $\alpha$ ) conditional mutants are identical and both mutants result in cell wall destabilization and defective organization of actin. Overexpression of *STT4* (PI4KIII $\alpha$ ) also suppresses the temperature-sensitive growth defect observed in *YPP1* (*TTC7*) mutants<sup>17</sup>. The role of *TTC7A* in PI4KIII $\alpha$  recruitment to the plasma membrane was also recently confirmed in mammalian cell lines<sup>24</sup> and we demonstrate for the first time that *TTC7A* and PI4KIII $\alpha$  directly interact in human cell lines. Since *TTC7A* is required for proper localization of PI4KIII $\alpha$  at the plasma membrane<sup>24</sup>, we propose that *TTC7A* mutations result in disease through loss of PI4KIII $\alpha$  at the plasma membrane and subsequent reduction of PIP that is required for cell polarity and survival. In support of this model, down-regulation of PI4KIII $\alpha$  results in increased apoptosis<sup>25</sup>, and furthermore intestinal specific murine knockout of *Pi4kca* (PI4KIII $\alpha$ ) results in a strikingly severe intestinal phenotype with widespread mucosal epithelial degeneration<sup>26</sup> reminiscent of our patients with *TTC7A* mutations. Therefore, our results demonstrate a direct interaction between PI4KIII $\alpha$ -*TTC7A*. And similar to the phenotype observed in *TTC7A*-deficient patients, *TTC7A* knockdown in human intestinal-like cell lines resulted in decreased adhesion, increased apoptosis. These results indicate that disruption of PI4KIII $\alpha$ -*TTC7A* pathway results in a combined T-cell and enterocyte defect that results in the intestinal phenotype described here (Figure 6).

The EFR3 homolog B (*EFR3B*; ENSG00000084710) gene product EFR3B tethers *TTC7A* (and *TTC7B*) to the plasma membrane and is essential for both *TTC7A* and PI4KIII $\alpha$  function<sup>24</sup>. Furthermore, knockdown of *EFR3B* results in the loss of both *TTC7A* and PI4KIII $\alpha$  at the plasma membrane and is critical for PI4KIII $\alpha$  signaling<sup>24</sup>. Interesting several *EFR3B* SNPs located both in the *EFR3B* gene and its flanking regions were reported to be associated with Crohn's Disease (<http://www.ibdgenetics.org> Supplemental Table 5; lead SNP rs1077492;  $p = 1.9 \times 10^{-14}$ , OR = 1.11). This locus on chromosome 2 at 25.12 Mb was recently reported in the IIBDGC meta-analysis as an IBD locus<sup>27</sup>. In-silico analyses



carried out by the IBDGC suggested ADCY3 as a potential candidate at this locus<sup>27</sup>; however, EFRB3's role in regulating PI4KIII $\alpha$ -TTC7A implicates *EFRB3* as a plausible causative IBD gene at this locus and that this PI4KIII $\alpha$ -TTC7A-EFRB3 pathway plays a broader role in adult-onset IBD.

Mutations in a *Ttc7a* TPR domain<sup>28–30</sup> result in flaky skin (*fsn*) mice and the associated pleiotropic abnormalities, including severe weight loss, with diarrhea and intestinal apoptosis being reported infrequently<sup>31, 32</sup>. Moreover, the intestinal specific knockout of *Pi4kca* (PI4KIII $\alpha$ ) in mice resulted in a severe intestinal phenotype with widespread mucosal epithelial degeneration<sup>26</sup>. The intestinal phenotype observed in these two mice models is reminiscent of the phenotype seen in our infantile patients who had massive shedding of enterocytes with increased apoptosis; however none of the patients developed psoriasis or other skin abnormalities as the *fsn*-mice. *TTC7A* has been investigated in human psoriasis and found not to be associated with human dermatological disease<sup>30</sup>. Thus psoriasis may only be observed in the *fsn* mice and may not be part of the human disorder.

We have shown that *TTC7A* is expressed in enterocytes and has a role in enterocyte survival and function suggesting that the physiological abnormalities observed in both mice and humans with *TTC7A* mutations results, at least in part, from epithelial dysfunction. However, as Chen et al<sup>11</sup> also demonstrated *TTC7A* is expressed in the thymus with marked reduction of thymocytes and lymphoid depletion in one patient with *TTC7A*-deficiency, *TTC7A* plays a critical role in modulating immune homeostasis and the immune deficiency also contributes to the pathogenesis of *TTC7A*-deficiency as seen in Families-1 and -2. These results are consistent with those seen in the MIA patients described with SCID<sup>11, 12, 33</sup> and points to a severe defect in both enterocyte and T-cell function; however, patients from Family-3 did not have an overt T-cell defect and patients with MIA described in<sup>11, 12, 33</sup> had varying degrees of immunodeficiency with some patients exhibiting mild T-cell lymphopenia in Chen et al<sup>11</sup> who also suggested that a enterocyte defect based on the high frequency of blood stream infections with intestinal microbes.

Therefore our studies further suggest that mutations in the *TTC7A*-deficiency can result in a spectrum of intestinal disease ranging from VEOIBD with apoptotic enterocolitis, as first described here, to MIA with SCID as described here and previously<sup>11, 12, 33</sup>. In support of this, *TTC7A* mutations were found to cause hereditary MIA with SCID<sup>11, 12, 33</sup>; however apoptotic enterocolitis has not been reported. The patients from Family-1 and -3, with apoptotic enterocolitis with no evidence on autopsy of MIA or stricturing disease, had mutations that would be predicted to reduce *TTC7A* expression but not completely abolish function. In support, we also demonstrated that the mutations identified in Families-1 and -3 reduced *TTC7A* binding to PI4KIII $\alpha$ . Therefore it is possible that the disease observed in patients from Families-1 and -3 represents a hypomorphic state where some residual *TTC7A* activity in both enterocytes and the thymus results in the severe enterocolitis without MIA and with/without lymphopenia.

All *TTC7A*-deficiency patients, including the patients described here, either died in infancy due to their progressive bowel disease, failed allogeneic hematopoietic stem cell transplantation, or survived with short gut and total parenteral nutrition (TPN)<sup>11, 12</sup>.

Interestingly, both Chen et al<sup>11</sup> and Samuels et al<sup>12</sup> described a MIA *TTC7A*-deficiency patient who had hematopoietic stem cell transplant and developed severe recurrence of MIA post transplant. The recurrence of MIA after resection in our Family-2 patients and those presented in <sup>11, 12</sup> suggests that *TTC7A*-deficiency results in a severe intestinal inflammatory process driven by a combined epithelial and T-cell defect that continues post-resection of atretic regions, and the enterocyte defect will not respond to hematopoietic stem cell transplant. Therefore, as we have demonstrated that an enterocyte defect is also found in patients with *TTC7A*-deficiency, transplantation of allogeneic hematopoietic stem cells may not be warranted in *TTC7A*-deficient patients. However, our study opens the possibility of pharmacologically targeting the PI4KIII $\alpha$ -*TTC7A*-EFR3B pathway as a potential therapeutic approach. The identification of *TTC7A* as a candidate gene for a unique and unrecognized variant of severe apoptotic enterocolitis further expands the genetic diversity of VEOIBD and the need to tailor therapeutic approaches for individual subtypes.

## Supplementary Material

Refer to Web version on PubMed Central for supplementary material.

## Acknowledgments

The authors thank the families of the patients described here from Canada, Germany, and Iran. A.M.M. is supported by an Early Researcher Award from the Ontario Ministry of Research and Innovation and funded by a Canadian Institute of Health Research – Operating Grant (MOP119457). S.B.S is supported by NIH Grants HL59561, DK034854, and AI50950 and the Wolpov Family Chair in IBD Treatment and Research. SP is supported by Lupus Research Institute Novel Grant Program and USM MEIF Development Grant program. This work was supported by DFG SFB1054, the Gottfried-Wilhelm-Leibniz program, BaySysNet (CK) and the Care-for-Rare Foundation (EB, DK). IBD Research at Cedars-Sinai is supported by USPHS grant PO1DK046763 and the Cedars-Sinai F. Widjaja Foundation Inflammatory Bowel and Immunobiology Research Institute Research Funds. Genotyping at CSMC is supported in part by the National Center for Research Resources (NCRR) grant M01-RR00425, UCLA/Cedars-Sinai/Harbor/Drew Clinical and Translational Science Institute (CTSI) Grant (UL1 TR000124-01), the Southern California Diabetes and Endocrinology Research Grant (DERC) (DK063491). In addition D.P.B.M. is supported by The Helmsley Foundation, The European Union, the Crohn's and Colitis Foundation of America, The Joshua L. and Lisa Z. Greer Chair in IBD Genetics. Subject ascertainment and data and sample processing was also supported by DK062413 and DK084554 and supplements to activities of the NIDDK IBD Genetics Consortium. This work was funded in part by a Helmsley Foundation grant to AMM, SBS, CK, DPBM, FP, and ES.

## References

1. Muise AM, Snapper SB, Kugathasan S. The age of gene discovery in very early onset inflammatory bowel disease. *Gastroenterology*. 2012; 143:285–8. [PubMed: 22727850]
2. Griffiths AM. Specificities of inflammatory bowel disease in childhood. *Best Pract Res Clin Gastroenterol*. 2004; 18:509–23. [PubMed: 15157824]
3. Heyman MB, Kirschner BS, Gold BD, et al. Children with early-onset inflammatory bowel disease (IBD): analysis of a pediatric IBD consortium registry. *J Pediatr*. 2005; 146:35–40. [PubMed: 15644819]
4. Glocker EO, Kotlarz D, Boztug K, et al. Inflammatory bowel disease and mutations affecting the interleukin-10 receptor. *N Engl J Med*. 2009; 361:2033–45. [PubMed: 19890111]
5. Kotlarz D, Beier R, Murugan D, et al. Loss of interleukin-10 signaling and infantile inflammatory bowel disease: implications for diagnosis and therapy. *Gastroenterology*. 2012; 143:347–55. [PubMed: 22549091]
6. Glocker EO, Frede N, Perro M, et al. Infant colitis--it's in the genes. *Lancet*. 376:1272. [PubMed: 20934598]

7. Worthey EA, Mayer AN, Syverson GD, et al. Making a definitive diagnosis: successful clinical application of whole exome sequencing in a child with intractable inflammatory bowel disease. *Genet Med.* 13:255–62. [PubMed: 21173700]
8. Blaydon DC, Biancheri P, Di WL, et al. Inflammatory skin and bowel disease linked to ADAM17 deletion. *N Engl J Med.* 365:1502–8. [PubMed: 22010916]
9. Matute JD, Arias AA, Wright NA, et al. A new genetic subgroup of chronic granulomatous disease with autosomal recessive mutations in p40 phox and selective defects in neutrophil NADPH oxidase activity. *Blood.* 2009; 114:3309–15. [PubMed: 19692703]
10. Muisse AM, Xu W, Guo CH, et al. NADPH oxidase complex and IBD candidate gene studies: identification of a rare variant in NCF2 that results in reduced binding to RAC2. *Gut.* 61:1028–35. [PubMed: 21900546]
11. Chen R, Giliani S, Lanzi G, et al. Whole-exome sequencing identifies tetratricopeptide repeat domain 7A (TTC7A) mutations for combined immunodeficiency with intestinal atresias. *J Allergy Clin Immunol.* 2013
12. Samuels ME, Majewski J, Alirezaie N, et al. Exome sequencing identifies mutations in the gene TTC7A in French-Canadian cases with hereditary multiple intestinal atresia. *J Med Genet.* 2013; 50:324–9. [PubMed: 23423984]
13. Krieger JR, Taylor P, Gajadhar AS, et al. Identification and selected reaction monitoring (SRM) quantification of endocytosis factors associated with Numb. *Mol Cell Proteomics.* 2013; 12:499–514. [PubMed: 23211419]
14. Dixon AL, Liang L, Moffatt MF, et al. A genome-wide association study of global gene expression. *Nature genetics.* 2007; 39:1202–7. [PubMed: 17873877]
15. Zhang B, Horvath S. A general framework for weighted gene co-expression network analysis. *Stat Appl Genet Mol Biol.* 2005; 4:Article17. [PubMed: 16646834]
16. Baird D, Stefan C, Audhya A, et al. Assembly of the PtdIns 4-kinase Stt4 complex at the plasma membrane requires Ypp1 and Efr3. *J Cell Biol.* 2008; 183:1061–74. [PubMed: 19075114]
17. Zhai C, Li K, Markaki V, et al. Ypp1/YGR198w plays an essential role in phosphoinositide signalling at the plasma membrane. *Biochem J.* 2008; 415:455–66. [PubMed: 18601652]
18. Begue B, Verdier J, Rieux-Laucat F, et al. Defective IL10 signaling defining a subgroup of patients with inflammatory bowel disease. *Am J Gastroenterol.* 2011; 106:1544–55. [PubMed: 21519361]
19. Engelhardt KR, Shah N, Faizura-Yeop I, et al. Clinical outcome in IL-10- and IL-10 receptor-deficient patients with or without hematopoietic stem cell transplantation. *J Allergy Clin Immunol.* 2012
20. Moran CJ, Walters TD, Guo CH, et al. IL-10R polymorphisms are associated with very-early-onset ulcerative colitis. *Inflamm Bowel Dis.* 2012
21. Cortajarena AL, Regan L. Ligand binding by TPR domains. *Protein Sci.* 2006; 15:1193–8. [PubMed: 16641492]
22. D'Andrea LD, Regan L. TPR proteins: the versatile helix. *Trends Biochem Sci.* 2003; 28:655–62. [PubMed: 14659697]
23. Flower TR, Clark-Dixon C, Metoyer C, et al. YGR198w (YPP1) targets A30P alpha-synuclein to the vacuole for degradation. *J Cell Biol.* 2007; 177:1091–104. [PubMed: 17576801]
24. Nakatsu F, Baskin JM, Chung J, et al. PtdIns4P synthesis by PI4KIIIalpha at the plasma membrane and its impact on plasma membrane identity. *J Cell Biol.* 2012; 199:1003–16. [PubMed: 23229899]
25. Ma H, Blake T, Chitnis A, et al. Crucial role of phosphatidylinositol 4-kinase IIIalpha in development of zebrafish pectoral fin is linked to phosphoinositide 3-kinase and FGF signaling. *J Cell Sci.* 2009; 122:4303–10. [PubMed: 19887586]
26. Vaillancourt FH, Brault M, Pilote L, et al. Evaluation of phosphatidylinositol-4-kinase IIIalpha as a hepatitis C virus drug target. *J Virol.* 2012; 86:11595–607. [PubMed: 22896614]
27. Jostins L, Ripke S, Weersma RK, et al. Host-microbe interactions have shaped the genetic architecture of inflammatory bowel disease. *Nature.* 2012; 491:119–24. [PubMed: 23128233]
28. White RA, McNulty SG, Nsumu NN, et al. Positional cloning of the Ttc7 gene required for normal iron homeostasis and mutated in hea and fsn anemia mice. *Genomics.* 2005; 85:330–7. [PubMed: 15718100]

29. Takabayashi S, Iwashita S, Hirashima T, et al. The novel tetratricopeptide repeat domain 7 mutation, *Ttc7fsn-Jic*, with deletion of the TPR-2B repeat causes severe flaky skin phenotype. *Exp Biol Med (Maywood)*. 2007; 232:695–9. [PubMed: 17463167]
30. Helms C, Pelsue S, Cao L, et al. The Tetratricopeptide repeat domain 7 gene is mutated in flaky skin mice: a model for psoriasis, autoimmunity, and anemia. *Exp Biol Med (Maywood)*. 2005; 230:659–67. [PubMed: 16179734]
31. Sundberg JP, France M, Boggess D, et al. Development and progression of psoriasiform dermatitis and systemic lesions in the flaky skin (*fsn*) mouse mutant. *Pathobiology*. 1997; 65:271–86. [PubMed: 9459497]
32. Ursina Nüesch, RS.; Schmid, Jana Pachlopnik. Clinical and histological features of flaky skin (*fsn*) mice. XXIX Meeting of the Swiss Immunology PhD students; 2012.
33. Bigorgne AE, Farin HF, Lemoine R, et al. TTC7A mutations disrupt intestinal epithelial apicobasal polarity. *J Clin Invest*. 2013

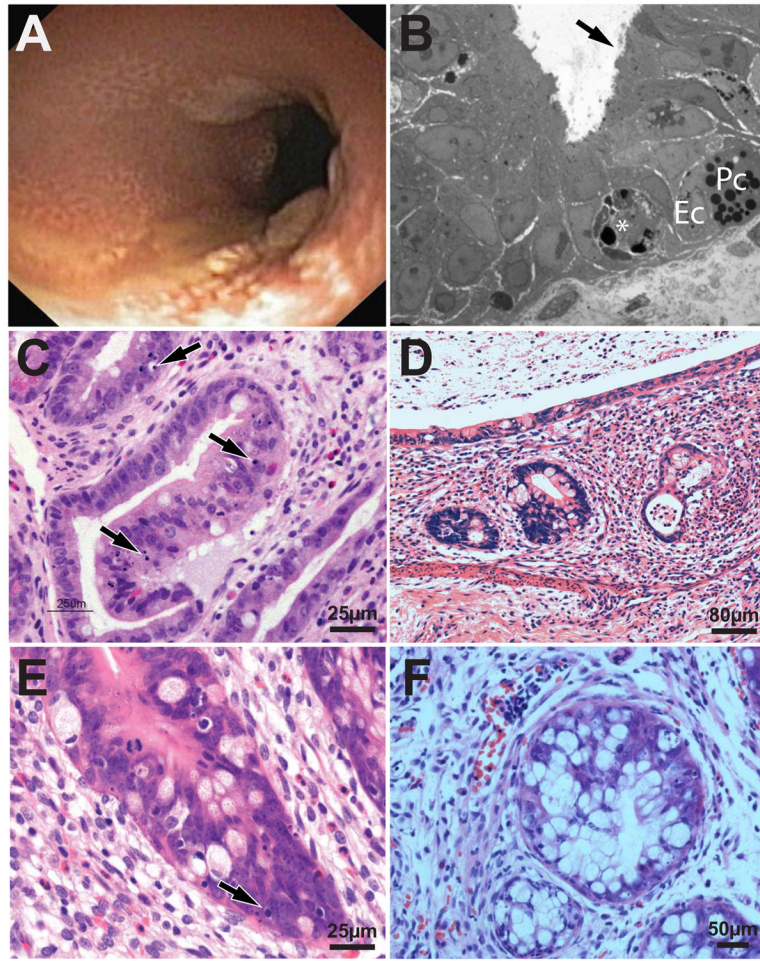


**Figure 1. Histological and Endoscopic Characteristics of Intestine of Patients with *TTC7A* Mutations**

**Figure 1A.** Colonoscopy showed severe inflammation characterized by continuous grade 2 colitis and multiple areas of exfoliation and sloughing of the surface epithelium from Family-1.

**Figure 1B.** Low magnification electron micrograph of crypt epithelium from the same biopsy as shown in C from Family-1. Amongst regenerating crypt cells, apoptotic cell (\*), enteroendocrine cell (EC) and Paneth cell (PC) is present. Crypt enterocytes showed sparse brush border microvilli (arrow) (Scale bar 10  $\mu$ m).

**Figure 1C.** High magnification of duodenal crypt epithelium showed extensive apoptosis from Family 1 (arrows) (H & E stain; Scale bar on Figure).

**Figure 1D–E.** Low (E) and High (F) magnification of Cecum epithelium showed extensive apoptosis from Family-2 (arrows) (H & E stain).

**Figure 1F.** High (F) magnification of Cecum epithelium showed extensive apoptosis from Family-3 (H & E stain).

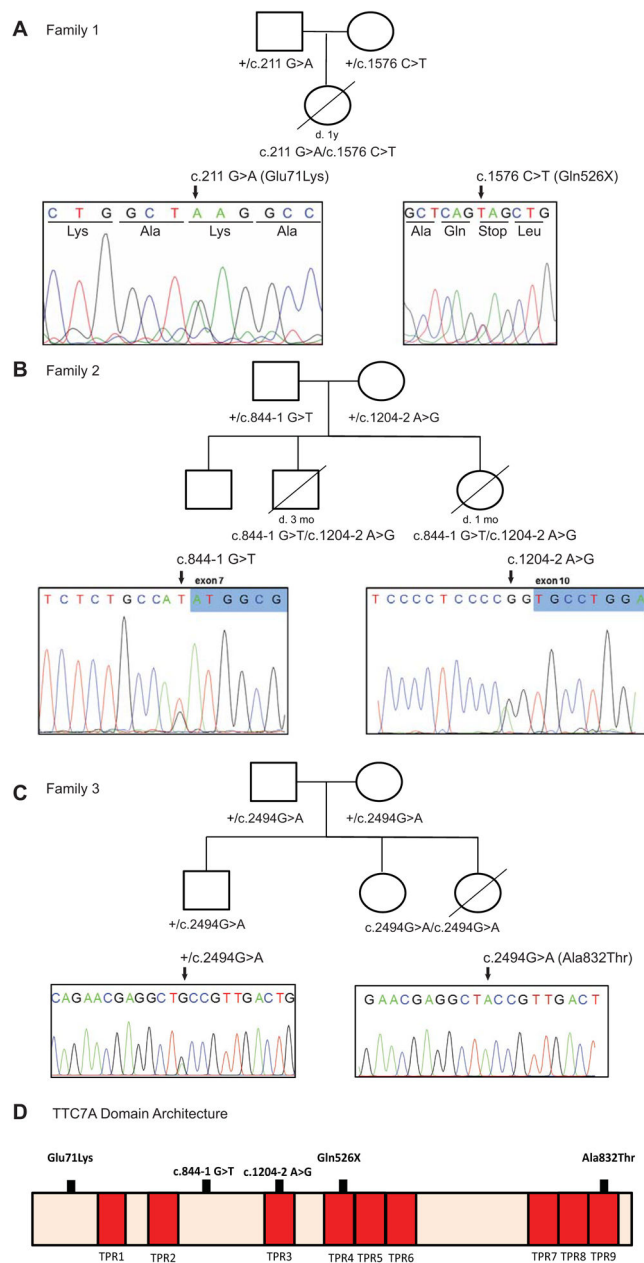


**Figure 2. *TTC7A* Genetic Analysis**

Figure 2A. Pedigree and *TTC7A* Mutations in Family-1.

Patient from Family 1 was heterozygous for 211G>A (p.E71K) inherited from her father and c.1944 C>T (p.Q526X) inherited from her mother.

Figure 2B. Pedigree and *TTC7A* Mutations in Family-2.

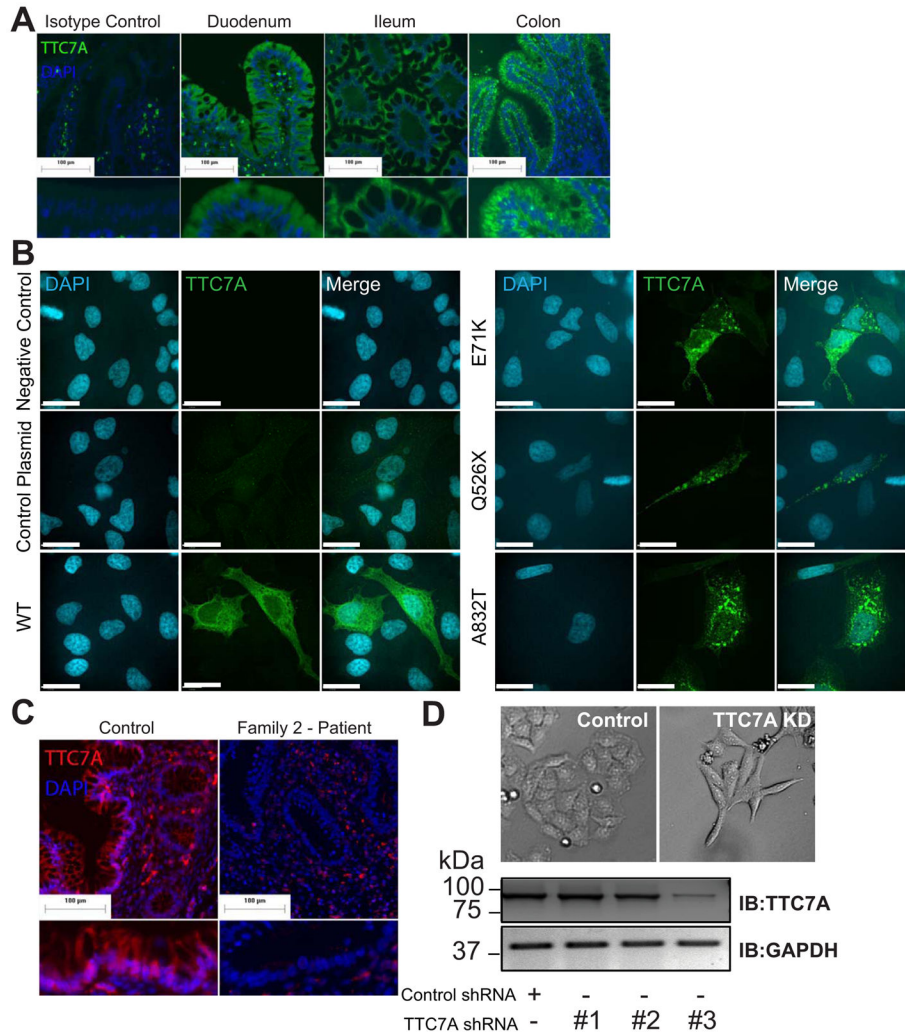
Siblings from Family 2 were heterozygous for a novel c.844-1 G>T *TTC7A* mutation in splice acceptor site of exon 7 inherited from the mother and a novel c.1204-2 A>G *TTC7A* mutation in splice acceptor site of exon 10 inherited from the father. A third sibling was found to be negative for both mutations.

Figure 2C. Pedigree and *TTC7A* Mutations in Family-3.

Siblings from Family 2 were homozygous for a non-synonymous mutation in exon 20 at c.G2494A resulted in a alanine acid to threonine substitution at amino acid position 832 (p.A832T).

Figure 2D. Location of TTC7A Mutations in Patients.

Cartoon of TTC7A protein with TPR domains in red and identified mutations highlighted.



**Figure 3. Functional TTC7A Enterocyte Studies**

Figure 3A. TTC7A Expression in Intestinal Enterocytes.

Immunofluorescence microscopy performed on human tissue sections immunostained using anti-TTC7A antibody (and DAPI) demonstrates TTC7A expression in enterocytes within the duodenum, ileum and colon. Lower inset panels represent zoomed images of the corresponding panel above. Scale bars = 100 μm.

Figure 3B. E71K, Q526X and A832T Mutations in TTC7A.

Caco-2 cells were transiently transfected with Myc-tagged wild-type, E71K, Q526X, and A832T TTC7A, immunostained using anti-Myc antibody and visualized using confocal microscopy. Negative control panels represent staining with secondary antibody only. The control plasmid represents an empty vector sham transfection. Scale bars = 25μm.

Figure 3C. TTC7A in Enterocytes from Patient Cecum (Family 2)

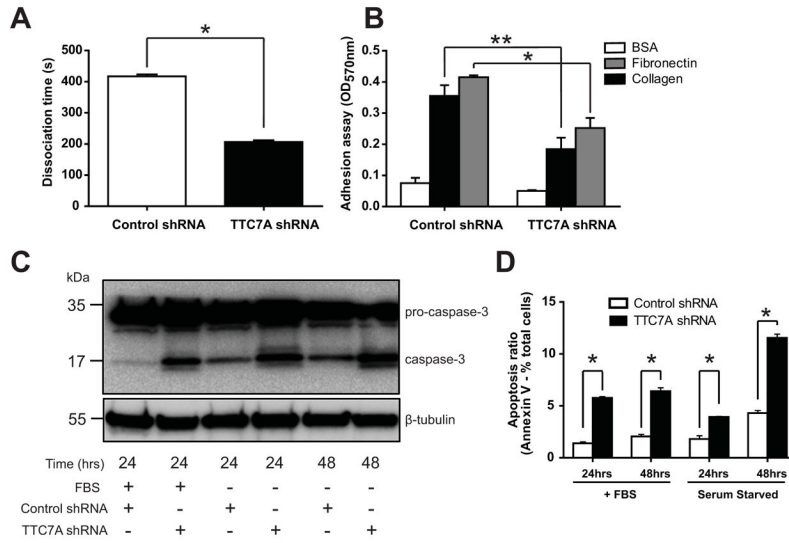
Immunofluorescence microscopy was performed on TTC7A-immunostained (and DAPI) cecal tissues sections from both control and patient (Family 2) biopsies. Compared to control staining (left panel), TTC7A expression is reduced in the patient sample (right panel). Scale bar = 100μm.

Figure 3D. Stable knockdown of *TTC7A* Resulted in Morphological Changes in Henle-407 cells.

Expression of TTC7A in stably transfected Henle-407 cells was reduced (70–80%) compared to Henle-407 cells stably transfected with control shRNA. The impact on cellular morphology of control and *TTC7A* shRNA knockdown was examined in



Henle 407 cells by contrast microscopy (100X magnification) under normal culture conditions. Knockdown of TTC7A resulted in a loss of cobblestone morphology and development of fibroblastoid morphology with spindle-like features.



**Figure 4.**

Figure 4A. Impaired Cell Adhesion in TTC7A-depleted Cells.

The total dissociation time, defined as the time required for complete dissociation of all cells from the tissue culture plate, was markedly reduced in TTC7A-depleted Henle-407 cells compared to control cells. Dissociation Assay (N=6 biological replicates, Student's t-test,  $p = 0.0022$ )

Figure 4B. Impaired Cell Adhesion to Collagen and Fibronectin in TTC7A-depleted cells.

Cell adhesion assays were performed using crystal violet staining. Control and TTC7A-depleted Henle 407 cells were seeded on 96 well plates coated with either collagen or fibronectin. Adhesion was assessed on the basis of optical density (OD) at 570nm.

N=3, (\*) Adhesion Assay N=3 biological replicates, Student's t-test,  $p(\text{Collagen}) = 0.027$  and  $p(\text{Fibronectin}) = 0.0077$

Figure 4C. TTC7A-depletion in Henle 407 Cells Results in Greater Caspase-dependent Apoptosis.

To investigate the impact of TTC7A suppression on the induction of apoptosis, the activation of caspase-3 was measured by western blot. Specific cleavage of pro-caspase 3 (32 kDa) into the active caspase-3 fragments (17k Da) was increased in cells serum-starved for 24 and 48 hours. N = 3, (\*)  $p = 0.012$ , ANOVA

Figure 4D. TTC7A-depletion in Henle 407 Cells Results in Greater Apoptosis Measured by Flow Cytometric Analysis of Annexin V.

To examine the significance of TTC7A suppression, following loss of attachment, flow cytometric analysis was conducted to quantify the extent of apoptosis in cells starved for 24 and 48 hours. Cells were stained with AnnexinV-PE and 7-AAD (viability marker); apoptotic cells were identified as AnnexinV<sup>+</sup> 7-AAD<sup>-</sup> cells. In TTC7A-depleted cells, the proportion of cells in early apoptosis increased to approximately 4.5% at 24 hours and 11.2% at 48 hours of serum-starvation compared to 1.3% (24 hours) and 4.1% (48 hours) in control cells.

Annexin V Apoptosis Assay N=3 biological replicates, Student's t-test,  $p(\text{FBS}, 24\text{h}) = 0.0018$ ,  $p(\text{FBS}, 48\text{h}) = 0.0076$ ,  $p(\text{SS}, 24) = 0.021$ ,  $p(\text{SS}, 48\text{h}) = 0.0034$

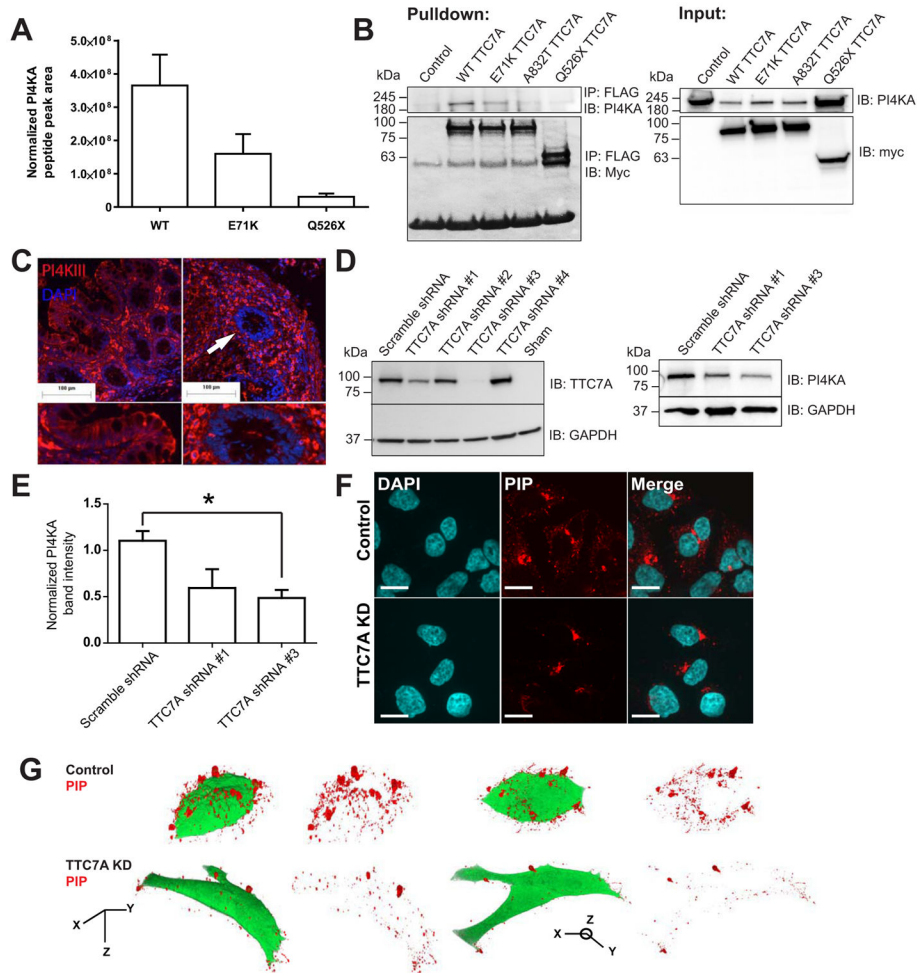


**Figure 5.**

Figure 5A. Tandem Mass Spectrometry.

E71K and Q526X mutations reduce the ability of TTC7A to immunoprecipitate PI4KA. Selected peptides from PI4KA and TTC7A were analyzed to determine the area under their MS1 peaks to assess the relative abundance of each peptide. The PI4KA present in each sample was normalized to the total TTC7A in each technical replicate to allow comparisons among biological replicates (n=3). These normalized values were averaged over all experiments. Error bars represent the standard error.

Figure 5B. PI4KIIIα-TTC7A Co-immunoprecipitate.

HEK293T cells were transiently transfected with Myc-tagged wild type (WT-TTC7A), E71K, Q526X, and A832T TTC7A constructs. Lysates were immunoprecipitated with anti-Myc antibody, and then immunoblotted using anti-PI4KIIIα and anti-Myc (for TTC7A) antibodies. The control lane represents transfection with an empty vector.

Figure 5C. Expression and Localization of PI4KIIIα is Altered in Patients with TTC7A-Deficiency

Immunofluorescence microscopy was performed on both control and patient colonic tissue sections immunostained with anti-PI4KIIIα antibodies. In the left panel, immunohistochemistry demonstrated that PI4KIIIα is highly expressed in enterocytes and immune cells from healthy human intestine. Inset panel depicts zoomed view of Panel 1 demonstrating PI4KIIIα expression at the plasma membrane of enterocytes. In the patient tissues, immunohistochemistry demonstrated that PI4KIIIα is dysregulated in enterocytes. Inset panel (representing region indicated by white arrow) demonstrates loss of PI4KIIIα at the plasma membrane of enterocytes bordering the intestinal crypt. Scale bar = 100µm.

Figure 5D. shRNA-mediated knockdown of TTC7A expression leads to decreased PI4KIIIα levels

To test the efficacy of the TTC7A shRNA, Henle-407 cells were transiently co-transfected with wild-type TTC7A and the various knock-down constructs, labelled #1 through #4, including a scrambled shRNA control and sham transfection. shRNA #1 and #3 showed reduction in TTC7A expression (left panels). shRNA containing the same targeting sequences were used to lentivirally infect Henle-407 cells where expression of PI4KIII $\alpha$  was assessed in cell lysates by Western blot (right panels).

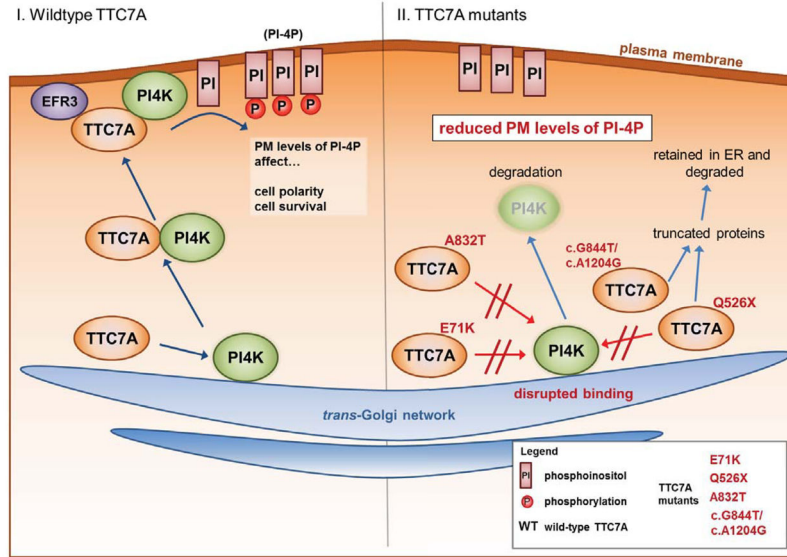
GAPDH was stained as loading control for all blots.

Figure 5E. Quantitation of PI4KIII $\alpha$  expression in Henle-407 cells infected with TTC7A shRNA.

Quantitation of Western blot band intensities from Figure 5D demonstrates a statistically significant reduction in PI4KIII $\alpha$  expression following TTC7A knockdown (Student's t-test, n = 3, p = 0.0234).

Figure 5Fi, Fii. TTC7A Depletion Results in Decreased PtdIns-4P (PI-4P) Production.

**(Fi – Cytoplasmic PIP)** TTC7A Knockdown and Control Henle-407 cells were stained with antibodies against PtdIns4P (in red; Z-P004, IgM, Cedarlane, USA) and DAPI (in blue) to visualize nuclei. **(Fii – Plasma Membrane PI-4P)** TTC7A knockdown Henle-407 cells have reduced plasma membrane immunostaining for PI-4P compared to controls. For control and TTC7A knockdown (KD), Henle-407 cells Z-stack images were generated at 0.2 $\mu$ m intervals and recapitulated using Volocity to generate a three-dimensional model to illustrate cell surface levels of PIP. Unconjugated GFP, expressed from the control and knockdown plasmids, was visualized and used to approximate the morphology of the cells. Each pair of images represents two views of the same cell according to axes depicted.



**Figure 6. Summary of TTC7 Mutations**

Schematic representation of the role of TTC7A in the trafficking of PI4KIII $\alpha$  to the plasma membrane from the *trans*-Golgi network. The left panel represents wild-type TTC7A in enterocytes wherein TTC7A binds to and facilitates the transport of PI4KIII $\alpha$  from the *trans*-Golgi to the plasma membrane. At the membrane, PI4KIII $\alpha$  can catalyze the production of PtdIns-4P(PI-4P). PI-4P levels at the plasma membrane have been implicated in cell survival and the maintenance of cell polarity. In the right panel, the various TTC7A mutations identified in the patients are depicted. E71K, Q526X and A832T TTC7A all demonstrated reduced binding to PI4KIII $\alpha$  which could reduce the interaction between TTC7A and PI4KIII $\alpha$ , hindering transport to the PM. Consequently, this will lead to reduced plasma membrane levels of PI-4P, a dysregulation that would affect downstream signaling pathways.

Table 1

Summary of *TTC7A* Mutations and Clinical Features

CS – Consanguinity (Y- yes, N- no), Total Parental Nutrition, AE - apoptotic enterocolitis.

	Age at Presentation	Gender	CS	Clinical Features	Immune Work-up	Outcome	<i>TTC7A</i> Mutation	<i>TTC7A</i> Mutated Protein
<b>Patient 1 (Family-1)</b>	At Birth	Female	N	Bloody Diarrhea; AE	Lymphopenia, hypogammaglobulinemia	Died at 11 months of age	c.211 G>A c.1944 C>T	p.E71K p.Q526X
<b>Patient 2 (Family-2)</b>	At Birth	Male	N	Obstruction, Stricture, AE	lymphopenia	Died at 3 months of age	c.844-1 G>T c.1204-2 A>G	Loss of the splice acceptor sites for exons 7 and 10
<b>Patient 3 (Family-2)</b>	At Birth	Female	N	Obstruction, Stricture, AE	lymphopenia	Died at 19 months of age	c.844-1 G>T c.1204-2 A>G	Loss of the splice acceptor sites for exons 7 and 10 respectively
<b>Patient 4 (Family-3)</b>	At Birth	Female	Y	Bloody Diarrhea; AE	Normal	Died at 11 month of age	c.2494 C>A	p.A832T
<b>Patient 5 (Family-3)</b>	At Birth	Female	Y	Bloody Diarrhea; AE	Normal	Alive, TPN for Partial Control	c.2494 C>A	p.A832T